European Polymer Journal 69 (2015) 284–295

Contents lists available at ScienceDirect

European Polymer Journal

journal homepage: www.elsevier.com/locate/europolj

Macromolecular Nanotechnology

Porous electrospun polycaprolactone (PCL) fibres by phase separation

Konstantinos Alexandros G. Katsogiannis, Goran T. Vladisavljević, Stella Georgiadou *

Department of Chemical Engineering, Loughborough University, Loughborough, Leicestershire LE11 3TU, UK

ARTICLE INFO

Article history:
Received 29 March 2014
Received in revised form 13 January 2015
Accepted 19 January 2015
Available online 28 January 2015

Keywords:
Nanofibres
Electrospinning
Polycaprolactone (PCL)
Phase separation
Porous fibres
Morphology

ABSTRACT

Porous electrospun poly(ε-caprolactone) (PCL) fibres were produced through a non-solvent induced phase separation mechanism, using binary solvent systems with different properties. The effect of the solvent properties on the size and surface morphology of electrospun PCL fibres was investigated. Chloroform (CF), dichloromethane (DCM), tetrahydrofuran (THF) and formic acid (FA) were used as good solvents in mixtures with a poor solvent, dimethyl sulfoxide (DMSO), in order to generate pores on the fibre surface. The production of porous, bead free fibres with an average diameter ranging from 1470 to 2270 nm was achieved using 12.5% *w*/*v* PCL in CF/DMSO solution with good/poor solvent ratios varying from 75% to 90% *v*/*v* at the applied voltage of 15 kV, a spinning distance of 20 cm, and the feed flow rate of 1 ml/h. DCM and THF were proven to be less suitable good solvents for the process due to the formation of a solid skin on the jet surface, caused by the limited diffusivity of the polymer molecules from the jet surface to the liquid core and its subsequent collapse. FA was found to be unsuitable due to its similar evaporation rate to DMSO. The pore formation was favoured at high good/poor solvent ratios, whereas, the production of fibres with ribbon cross sections or fibres with beads was more pronounced at low good/poor solvent ratios. Data fitting was used for the development of a second order polynomial equation, correlating the produced fibre average diameter to the solution parameters (conductivity, surface tension, and viscosity), for the given polymer and solvent systems, under the specific experimental conditions used in this study. The ternary mixture compositions that lead to the formation of porous fibres were mapped on a ternary graph.

1. Introduction

Electrospinning is a straightforward method that uses an external electric field to produce polymer fibres with diameters down to nanometre scale [8]. Electrospinning involves the acceleration of a charged jet of polymer solution towards a grounded collector. The solvent evaporation and the stretching of the jet, caused by the repulsive forces of the charged molecules within the jet, are responsible for the formation of the polymer fibres [6]. As a result of their small diameters, those fibres exhibit high surface area per volume ratio, which makes them excellent candidates for a wide range of applications [18], such as production of scaffolds for tissue engineering [21,3]. However, the requirements for these applications are not limited to the small size of the fibres. The role of the scaffolds is to mimic the behaviour of the extracellular matrix (ECM) and provide the appropriate environment for the cellular growth, therefore a porous fibrous structure is required in order to improve the cell attachment on the scaffold [23,26].

A plethora of methods has been developed in order to increase the porosity of electrospun fibres, such as electrospinning of polymer blends and subsequent removal of one

* Corresponding author. Tel.: +44 (0) 1509 222521.
E-mail address: S.Georgiadou@lboro.ac.uk (S. Georgiadou).

http://dx.doi.org/10.1016/j.eurpolymj.2015.01.028
0014-3057/

of the polymers [2], the use of bath collector [28], and the use of additives [11]. However, those methods lack simplicity, since they require post electrospinning treatment of the fibres, set up modifications and any residual additives might affect the quality of the fibres. The simplest methods that have been suggested for pore formation are the breath figures and the phase separation mechanisms. The breath figures mechanism was observed by Srinivasarao et al. [29], who first described the formation of pores on a polystyrene (PS) film in a humid environment. In that case the solvent evaporation caused a lowering of the temperature on the surface of the film. Water vapour from the atmosphere was condensed on the surface, leaving an imprint on the film. Finally, the pores were created by the evaporation of the water molecules from the surface. The use of humidity to increase the porosity of electrospun fibres has also been proposed by other researchers [4,12,25]. Phase separation is an alternative method that has been extensively used for the production of porous membranes for filtration applications [10], but it has not been fully explored yet for electrospinning, as very limited work has been reported for the formation of porous polyacrylonitrile and polymethacrylate fibres. [24]. Phase separation occurs when a polymer solution becomes thermodynamically unstable and separates into polymer rich and polymer poor phases. The precipitation of the polymer from the polymer-rich phase forms the matrix, whereas the pores are formed from the polymer poor phase [7]. The thermodynamic instability can be caused either by the polymer, such as in the case of electrospinning amphiphilic copolymers [1] or by the solvent. Megelski et al. [22] investigated the phase separation mechanism during electrospinning of PS in a THF solution. They identified two different phase separation mechanisms responsible for the pore formation: Thermal Induced Phase Separation (TIPS), caused by lowering the temperature on the fibres due to solvent evaporation and Vapour Induced Phase Separation (VIPS), induced by absorption of water vapour from the atmosphere. A different approach involves the addition of non-solvent with higher boiling point than that of the good solvent, in the polymer solution prior to electrospinning (non-solvent induced phase separation, NIPS) [27,19,31,9]. The presence of a non-solvent can induce thermodynamic instability of the solution and initiate the phase separation process. An advantage of NIPS over the other phase separation mechanisms is that it can be controlled and can provide reproducible results.

The aim of this study was to investigate the formation of porous electrospun poly(ε-caprolactone) (PCL) fibres through a NIPS mechanism and the effect of different solvent systems' properties on the surface morphology and size of electrospun poly(ε-caprolactone) (PCL) fibres. PCL is a linear polyester, which has attracted an increasing interest in recent decades, due to its biodegradability and suitability for biomedical applications [32,15,16]. The design involved the use of solvent mixtures composed of good and poor solvents of PCL, in various ratios. Good solvents chosen in this work were chloroform (CF), dichloromethane (DCM), tetrahydrofuran (THF) and formic acid (FA). The first criterion for their selection was the ability of those solvents to produce electrospinnable solutions [20]. The second criterion was the wide range of physical properties and characteristics that those solvents possess. CF was used as a reference solvent, DCM was used due to its comparatively lower boiling point, THF was used due to its miscibility with water and FA has a higher boiling point and dielectric constant compared to the other good solvents. Dimethyl sulfoxide (DMSO) was selected as a poor solvent based on its high dielectric constant, which is essential for the fibre formation [20], its miscibility with all the good solvents and its high boiling point. The high boiling point of the poor solvent is essential for the phase separation to occur. The physical properties of the solvents used in this work are summarized in Table 1.

2. Experimental

2.1. Materials

PCL with average number molecular weight of 80,000 was purchased from Sigma–Aldrich. CF was ACS reagent, had purity ⩾99.8% and contained ethanol as a stabilizer. DCM was ACS reagent, with ⩾99.5% purity and contained amylene as a stabilizer. THF was ACS reagent, had purity ⩾99.0% and contained BHT as an inhibitor. DMSO was ACS reagent, had purity ⩾99.9%. FA was reagent grade and had purity ⩾95.0%. All the chemicals were used as delivered. All the solutions were prepared at room temperature and used within 4 h after their preparation. All the solvents were characterised based on the time required to produce a 10% *w*/*v* PCL solution. Good solvents were considered those able to produce a 10% *w*/*v* PCL solution within 2 h, as partial solvents were characterised those able to produce a 10% *w*/*v* PCL solution within 4 h and as poor solvents were characterised those unable to produce a 10% *w*/*v* PCL solution, even after 24 h. The results are shown in Table 1.

2.2. Electrospinning experiments

A horizontal electrospinning set-up was used for the experiments in this work. 20 ml of the solution were loaded in a plastic syringe and the syringe was placed on a syringe pump (PHD ULTRA, Harvard Apparatus). The electric potential was applied to the metallic needle (18 gauge, 1.270 mm outer diameter, 0.838 mm inner diameter, 3.2 cm length, Fisher Scientific) by the high voltage power supply (Series FC, Glassman High Voltage Inc.). The fibres were collected on a flat copper plate covered with aluminium foil. All the experiments were conducted at room temperature (17–22 °C) and a relative humidity of 30–40% within a closed chamber. The experimental conditions were kept constant for all the experiments. The applied voltage was 15 kV, the solution flow rate was 1 ml/h, the tip of the needle to collector distance was 20 cm and the duration of each experiment was 10 min.

2.3. Solution parameters characterisation

The conductivity was measured using a JENWAY 4071 conductivity metre. The surface tension was measured

Table 1
Properties of the solvents used in this work.

Solvent	Boiling point (°C)	Dielectric constant at 20 °C	Surface tension at 20 °C (mN/m)	PCL solubility
CF	61	4.8	27.2	Good
DCM	40	9.1	28.1	Good
THF	66	7.6	28.0	Good
FA	101	58.0	37.7	Partial
DMSO	189	46.6	43.7	Poor

using a White Elec Inst balance (model DB2kS). At least 5 measurements were performed for each sample, in order to obtain an average. The viscosity was measured using a Thermo Haake VT550 rotational viscometer.

2.4. Fibre morphology characterisation

Field emission scanning electron microscopy (FESEM, Carl Zeiss (Leo) 1530VP) was used for the characterisation of the surface morphology of the fibres. All the samples were sputter coated with gold (Q150T ES, Quorum) prior to their observation under the microscope. The diameter of the fibres was measured by AxioVision software. At least 100 fibre diameters were measured per sample, in order to ensure the accuracy of the measurements. The standard deviation of the fibre diameter and the coefficient of variation (ratio of standard deviation to the mean diameter), were calculated for all the samples. In the case of fibres with ribbon cross sections, the diameter refers to the width of the fibre.

3. Results and discussions

3.1. Solvent effect/solvent ratio effect

Four different good solvents were used in this study, in order to investigate their effect on the morphology and size of the obtained fibres. The polymer concentration was kept constant at 12.5% *w*/*v* for three of the solvents (CF, DCM, THF) and the amount of the good solvent within the solvent mixture was varied between 50% and 100% *v*/*v*, with an interval of 10% *v*/*v*. FA was examined separately, since the polymer concentration was reduced to 10% *w*/*v* and the only good/poor solvent ratio that was studied was 90% *v*/*v*, due to issues concerning the solubility of PCL in FA.

The properties of the feed solutions are shown in Fig. 1. As can be seen, the type of good solvent used did not significantly affect the surface tension of the feed solutions for any given good/poor solvent ratio (Fig. 1B). As expected, the addition of DMSO caused both the surface tension and the conductivity to increase for increasing DMSO amount or decreasing good/poor solvent ratio (Fig. 1A and B). The variations in the viscosity values (Fig. 1C) were caused by complex intermolecular interactions between polymer, good solvent and poor solvent.

The process can be better understood by taking into consideration the phenomena occurring after the jet ejection. The homogeneous, prior the jet ejection, solutions are subjected to constant composition changes. The

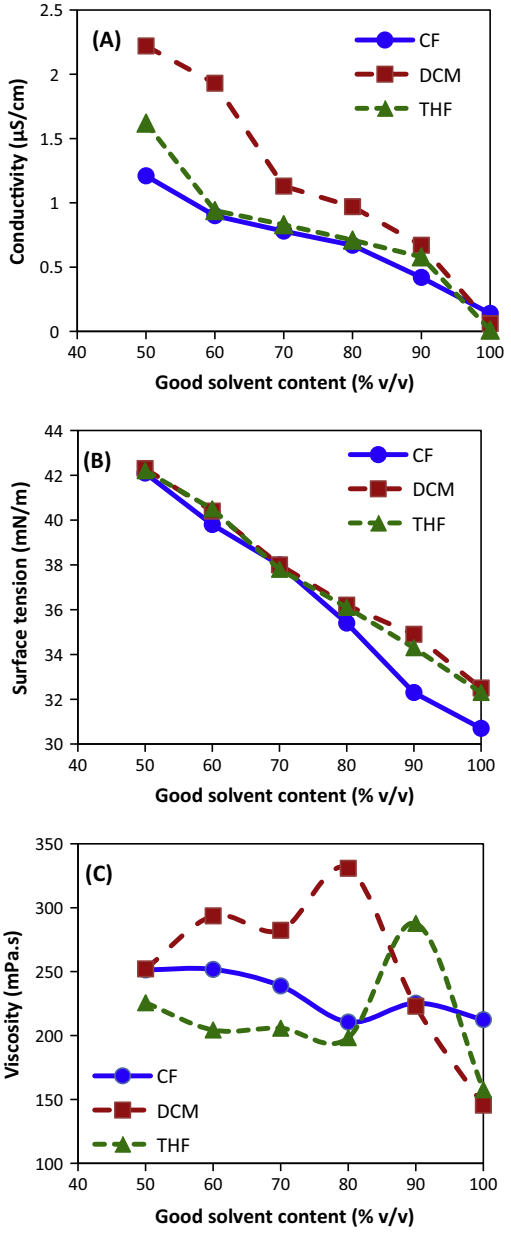

Fig. 1. Solution properties (A) conductivity, (B) surface tension, (C) viscosity for solutions with 12.5% *w*/*v* PCL concentrations and varying good/poor solvent ratios.

evaporation rate of the good solvent is higher than that of the poor solvent and therefore, the good/poor solvent ratio is progressively decreasing. The PCL concentration in the jet increases due to solvent loss. In addition to that, the solvent evaporation occurs mainly from the surface of the jet and the diffusion rate of solvent molecules from the core to the surface, or diffusion of polymer molecules from the jet surface to the core is usually lower than that of the solvent evaporation. Finally, the absorption and diffusion of water molecules from the atmosphere within the jet, alters the jet composition, as well. All the above mentioned phenomena, with varying levels of contribution, lead to the alteration of the jet composition, both, in general and in local features (i.e. formation of heterogeneous regions within the jet).

Fig. 2 shows the fibres produced from CF based solutions. The average diameters of the produced fibres and their coefficient of variation are summarized in Table 2. The morphological evolution of the fibres with increasing the amount of non-solvent was

Bead-on-string → Porous → Ribbon
→ Porous bead-on-string

Initially, the use of CF as a single solvent resulted in the production of non-porous fibres with bead-on-string morphology (Fig. 2A). This morphology could be caused by the low dielectric constant of chloroform. The addition of small amounts of non-solvent (10% and 20% *v*/*v*), however, modified the produced fibre morphology (Fig. 2B and C). The obtained fibres exhibited porous surface and the beads were eliminated due to the higher solution conductivity compared to pure CF. The higher evaporation rate of CF compared to that of DMSO alters the composition of the electrospinning jet during its travel, since a higher amount of CF evaporates compared to that of DMSO. The transition of the binary solvent system from the stable, one phase

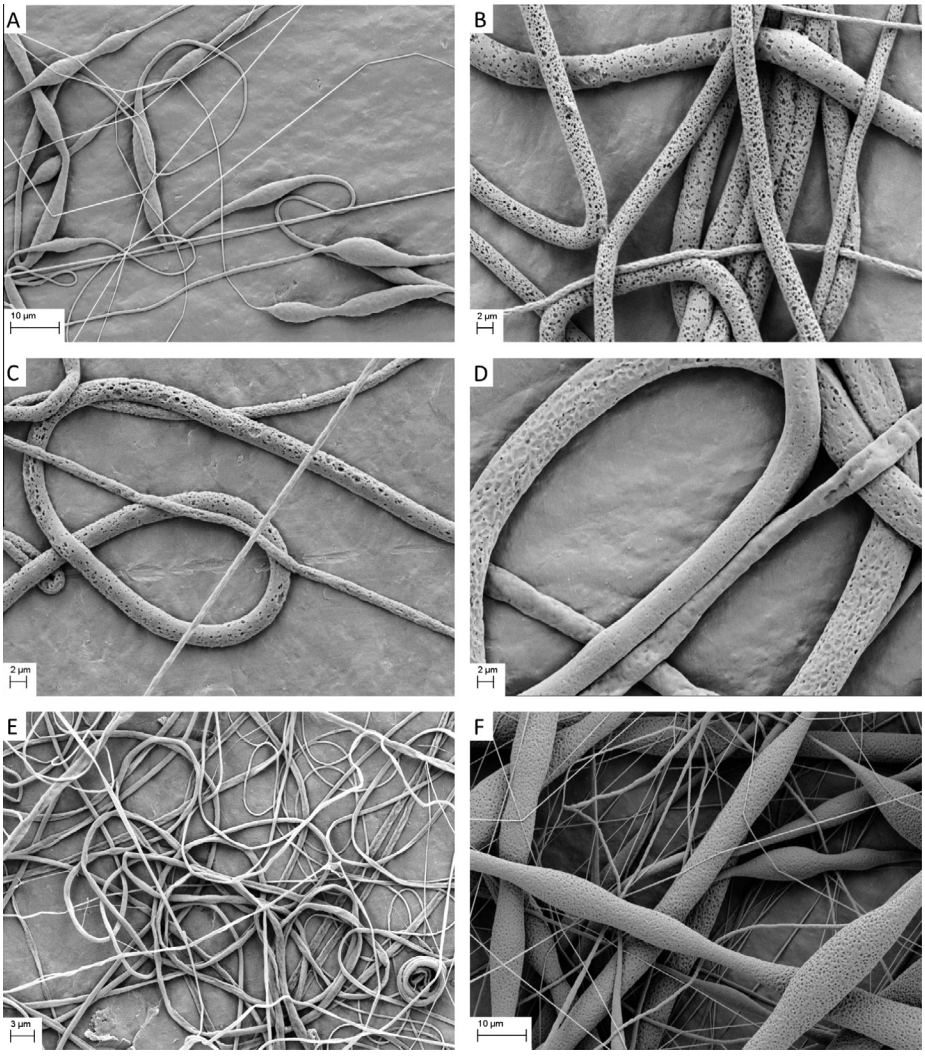

Fig. 2. SEM pictures of the fibres produced by CF/DMSO solutions. The polymer concentration in the feed solution was 12.5% *w*/*v* in all cases and the concentration of good solvent in the good/poor solvent mixture was: (A) 100% *v*/*v*, (B) 90% *v*/*v*, (C) 80% *v*/*v*, (D) 70% *v*/*v*, (E) 60% *v*/*v*, and (F) 50% *v*/*v*.

Table 2
Fibre average diameter and coefficient of variation for fibres produced by CF based solutions (* the diameter refers to the width of fibres with ribbon cross sections).

CF amount (% *v*/*v*)	Fibre average diameter (nm)	Coefficient of variation (%)
100	600	49
90	2270	35
80	1470	40
70	2120	67
60	650*	52
50	550	54

region to the unstable, two phase region causes the initiation of the phase separation mechanism. The surface morphologies of the produced fibres indicate the successful completion of the mechanism. The pores are irregularly shaped, have varying depth and wide size distribution, which are characteristics that accompany the structures produced by phase separation. The observed reduction of the fibre diameter from 2270 to 1470 nm accompanying the increase of the DMSO concentration in the electrospinning solution from 10% to 20% *v*/*v* as shown in Table 2 can be attributed to the increase of the conductivity of the solution from 0.42 to 0.67 μS/cm.

A further increase of the DMSO content in the initial solution, however, results in a different course of events. A tendency for pore elimination and transformation of circular cross sections to elliptical or ribbon is observed when the DMSO concentration in the feed solution is 30% *v*/*v* (Fig. 2D), and this tendency becomes more prevalent at higher DMSO concentrations (CF 60% *v*/*v* – Fig. 2E) with the production of fibres with smooth surface and ribbon cross sections. Fibres with similar morphologies have been reported previously [14] and this morphology is caused by the formation and subsequent collapse of a solid skin on the surface of the electrospinning jet. As mentioned before, the evaporation of the solvents occurs mainly from the surface of the jet. The diffusion of the remaining polymer molecules from the jet surface to the liquid core, however, is hindered by the increased amount of the less volatile non-solvent. The consequent polymer accumulation on the jet surface is responsible for the skin formation. The evaporation of the solvents from the liquid core continues to occur through the solid skin. When the core is not able to provide support to the skin, it collapses under forces applied on it by the atmospheric pressure.

Another interesting phenomenon is the presence of beads when the amount of DMSO was increased to 50% *v*/*v* (Fig. 2F). There are two possible explanations for this phenomenon. Wei et al. [31] adapted the theory that large non-solvent amounts can cause the formation of heterogeneous regions within the electrospinning jet. In this case, this formation is enhanced, since in the existing amount of non-solvent (DMSO) the addition of water by its absorption from the atmosphere should be taken into account. The different viscosities of those regions lead to the formation of fibres with different diameters. The presence of beads can be attributed to the presence of regions with low viscosities. A second explanation involves the subsequent increase of the surface tension after the water absorption. The water contribution can elevate the surface tension of the jet up to the point, where, it can prevail over the forces applied by the electric field, and, therefore, lead to bead formation.

Fig. 3 shows the fibres produced from DCM based solutions. The produced fibre average diameters and their coefficient of variation are summarized in Table 3. In the case of DCM based solutions, its higher volatility, compared to that of CF, seems to be the governing parameter that affects the produced fibre morphology. Even though the CF and DCM solutions have the same initial concentration, the higher evaporation rate of DCM results the formation of more dense jet compared to those of CF. The increased viscosity of the jet facilitates the formation of a solid skin on the jet surface, due to difficulties that the polymer chains are facing in their migration from the surface to the liquid core [5]. The morphological evolution of the fibres with increasing DMSO content was

Non porous → Porous fibres with beads
→ Wrinkled fibres → Ribbon
→ Bead-on-string

When DCM was used as a single solvent, the fibre morphology was a mixture of fibres with circular and ribbon cross sections. In contrast with the use of chloroform as a single solvent system, no beads were observed on the fibres. The bead absence can be attributed mainly to the higher DCM dielectric constant (9.1), and also to the higher evaporation rate and the subsequent increase of the solution concentration. The circular shape and the comparable sizes and depth of the observed pores on some fibres, indicate that they were rather produced by the breath figures mechanism than phase separation.

The variations, which are observed from the CF morphological evolution for the binary solvent systems, can be explained by the difference of CF and DCM evaporation rate as well. Low DMSO concentrations (10% *v*/*v*) were proven to be suitable for the formation of pores on the fibre surface, similarly to the CF based solutions. The presence of beads is the feature that differentiates the produced fibre morphologies in those cases. Two phenomena described above, the formation of heterogeneous regions within the jet and the increase of the jet surface tension following water absorption could be used as possible explanations for the bead formation. A further increase of the DMSO concentration (20% *v*/*v*) in the feed solution caused the formation of fibres with wrinkled surface. It is interesting to note that the diameter of these fibres is 2900 nm, due to higher solution viscosity. In that case a solid skin formed on the surface of the jet, however, since the large diameter of the fibres leads to longer drying time, the drying has not been completed and when their collapsing occurred they were in quasi solid state and, therefore, it was not uniform. The elongated shape of the pores supports that theory, since the stretching of the fibres continues to occur when they are at the quasi solid state. Complete drying of the fibre skin, in the cases where the DMSO amount in the feed solution was 30% and 40% *v*/*v*, was a result of the smaller fibre size (diameters 1030 and

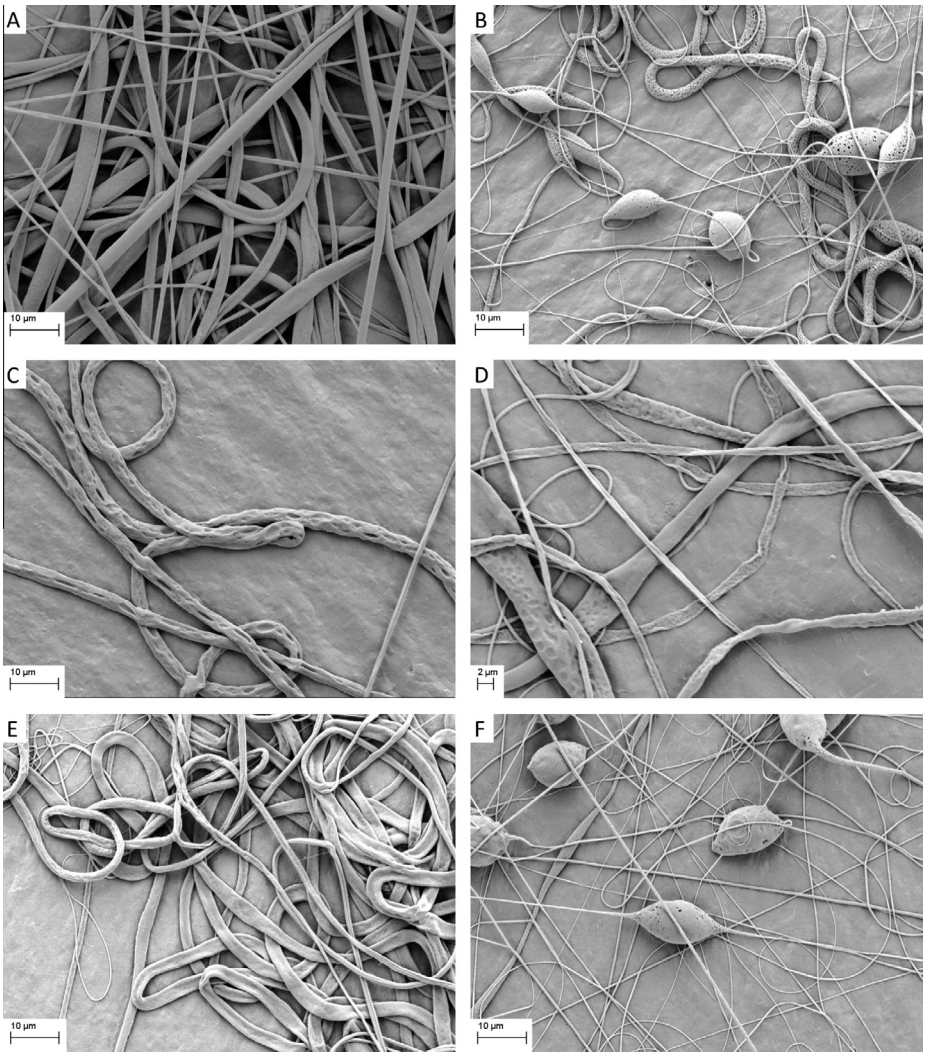

Fig. 3. SEM pictures of the fibres produced by DCM/DMSO solutions. The polymer concentration in the feed solution was 12.5% *w*/*v* in all cases and the concentration of good solvent in the good/poor solvent mixture was: (A) 100% *v*/*v*, (B) 90% *v*/*v*, (C) 80% *v*/*v*, (D) 70% *v*/*v*, (E) 60% *v*/*v*, and (F) 50% *v*/*v*.

Table 3
Fibre average diameter and coefficient of variation for fibres produced by DCM based solutions (* the diameter refers to the width of fibres with ribbon cross sections).

DCM amount (% *v*/*v*)	Fibre average diameter (nm)	Coefficient of variation (%)
100	1550	40
90	600	21
80	2900	26
70	1030*	53
60	2150*	36
50	470	38

2150 nm, respectively), and, hence, its uniform collapsing led to the production of fibres with ribbon cross sections. The beads that were observed when the non-solvent content was increased to 50% *v*/*v* could be attributed either to the formation of heterogeneous regions within the jet or to the subsequent increase of the surface tension after the water absorption.

Fig. 4 shows the fibres produced from THF based solutions. The produced fibre average diameters and their coefficient of variation are summarized in Table 4. In the case of THF based solutions, the key parameter is its miscibility with water. This miscibility enhances the absorption of larger amounts of water from the atmosphere, compared to other solvent systems, and also facilitates the diffusion of the water within the jet. The morphological evolution of the fibres with increasing DMSO content was

Non porous → Porous fibres with beads
→ Fibres with dimpled beads → Ribbon

The lack of beads that is observed when THF was used as a single solvent can be attributed to the relatively high dielectric constant of THF (7.6).

The addition of small amounts of DMSO (10% and 20% *v*/*v*) to the feed solutions resulted in the presence of beads on the produced fibres. In those cases, the evaporation of THF and, mainly, the simultaneous absorption of larger, compared to the CF and DCM based solutions, amounts of water, due to its miscibility with THF, contribute to the formation of heterogeneous regions within the jet, which could cause the bead formation. In support of that theory is the high normalised standard deviation of the produced fibre diameter (73%) for the solution where 10% *v*/*v* DMSO was added.

A further increase of the DMSO amount in the feed solution to 30% *v*/*v* or above, however, results in the predominant production of fibres with ribbon-shaped cross section. As mentioned before, the formation of a solid skin is the reason for those morphologies. In those cases the skin formation is favoured due to the presence of large amount of non-solvent, which hinders the diffusion of the polymer chains from the jet surface to the core. It should be noted that, besides the DMSO which was present in the initial solution, the larger amounts of the absorbed water will also enhance this phenomenon.

The significance of the THF miscibility with water is highlighted by a comparison of the produced fibre morphologies for the samples where the good solvent concentration was 50% *v*/*v*. In the case of THF, no beads are observed (Fig. 4F) in contrast to the observed morphologies for the CF and DCM based solutions (Figs. 2F and 3F, respectively). A possible explanation is that the water, which is absorbed by the atmosphere, is distributed more uniformly within the jet due to its miscibility with THF and the formation of heterogeneous regions, with different viscosities, is avoided. In support of that theory is the lower coefficient of variation of the fibre diameter that is observed for the THF based solution (34%) compared to the CF and DCM based solutions (54% and 38%, respectively).

A solution, were FA was the good solvent, was tested as well. FA is not as good solvent for PCL as CF, DCM and THF,

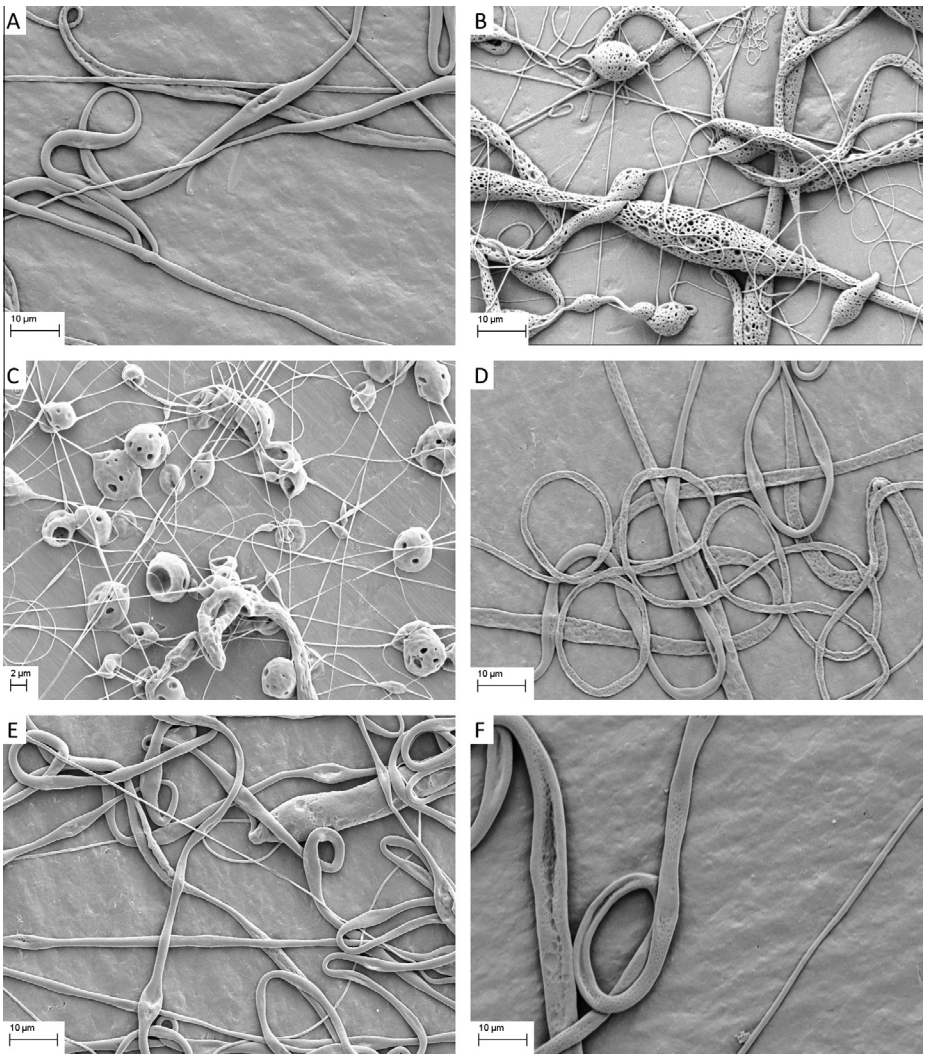

Fig. 4. SEM pictures of the fibres produced by THF/DMSO solutions. The polymer concentration in the feed solution was 12.5% *w*/*v* in all cases and the concentration of good solvent in the good/poor solvent mixture was: (A) 100% *v*/*v*, (B) 90% *v*/*v*, (C) 80% *v*/*v*, (D) 70% *v*/*v*, (E) 60% *v*/*v*, and (F) 50% *v*/*v*.

Table 4
Fibre average diameter and coefficient of variation for fibres produced by THF based solutions (* the diameter refers to the width of fibres with ribbon cross sections).

THF amount (% *v*/*v*)	Fibre average diameter (nm)	Coefficient of variation (%)
100	1460	35
90	900	73
80	280	24
70	1180*	52
60	1390	38
50	2412*	34

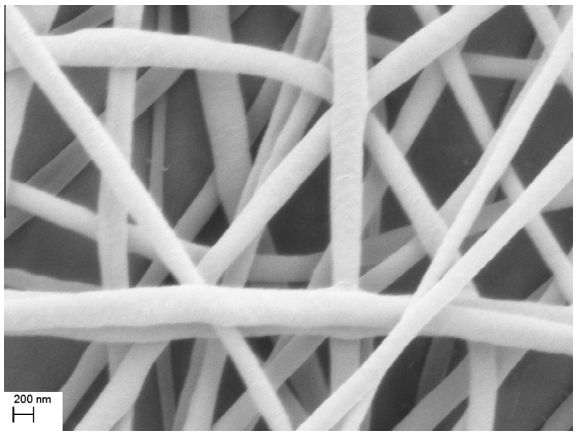

Fig. 5. SEM picture of fibres produced by a 10% *w*/*v* FA/DMSO solution. The good/poor solvent ratio was 90% *v*/*v*.

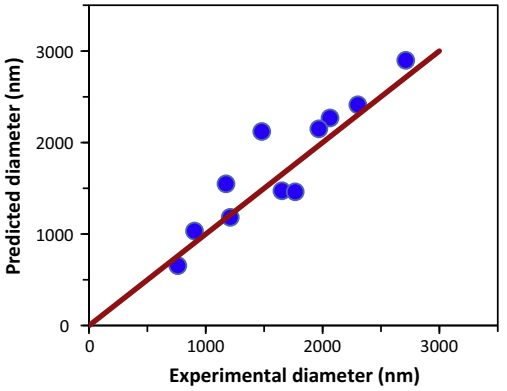

Fig. 6. Fitting of the experimental data in the empirical equation.

and, since it acts as a catalyst for the depolymerisation of PCL [17], the solution concentration and the poor/good solvent ratio were reduced. The ratio of good/poor solvent was 90% *v*/*v* and the concentration of the solution was 10% *w*/*v*. The fibres that were produced from that solution are shown in Fig. 5.

The produced fibres had a mean diameter of 250 nm and the coefficient of variation was 39%. The small size of the fibres was a result of the high dielectric constant of FA. The same trend has also been observed in other studies [13,30], where FA was used as a solvent in electrospinning of PCL. The most interesting observation however is the absence of pores on the surface of the fibres. FA has the highest boiling point, compared to the other good solvents used in this project. Since FA and DMSO have similar evaporation rates, the composition of the solvent mixture does not change enough to cause the instability required for the phase separation. This requirement for a distinct difference between the evaporation rates of the good and the poor solvent has been reported by Lubasova and Martinova [19] as well.

3.2. Empirical equation to relate solution properties to fibre diameter

To explore the relationship between the solution properties and the produced porous fibre diameters and to improve our understanding of their effect on fibre morphology, data fitting was used to obtain an empirical equation correlating the produced fibre mean diameter to some of the solution properties for the given polymer and solvent systems, and the specific process parameters (voltage and flow rates) used in this study. More specifically, the least squares method was used in order to fit the experimental data to a second order polynomial equation. Although numerous parameters affect the outcome of the electrospinning process, including the boiling point or vapour pressure of the solvent, the polymer molar mass and the humidity in the electrospinning chamber, the method used only allowed the analysis of a limited number of three variables. Hence the empirical modelling was implemented using only three solution parameters. The three independent variables selected were conductivity, surface tension, and viscosity, due to their importance in fibre formation and the best fitting of the data into an equation. Trials were also carried out using the boiling point as one of the three variables, however the fitting was poor and these results are not shown here. Of course, the complex interrelated processes involved in fibre formation cannot be described by using only three variables and

Table 5
Properties of the solutions used for equation testing.

Sample number	Good solvent	Good solvent concentration (% *v*/*v*)	Solution conductivity (μS/cm)	Solution surface tension (mN/m)	Solution viscosity (mPa s)
1	CF	75	0.73	36.9	228
2	DCM	75	1.01	37.5	285
3	DCM	83	0.79	35.9	252
4	THF	75	0.74	37.3	208
5	THF	83	0.73	35.9	217

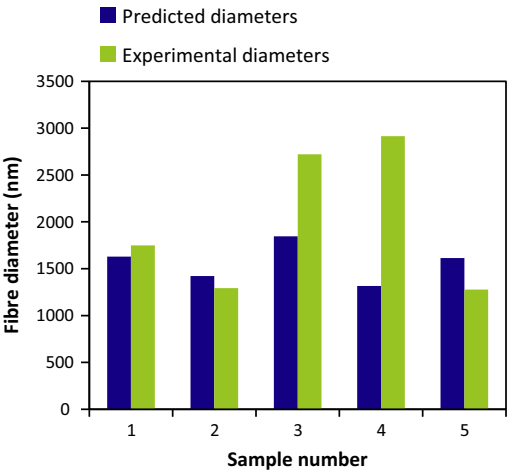

Fig. 7. Testing of the empirical equation.

the empirical equation produced is not universal, as for example, the coefficients of the equation would change if different solvent systems, polymer molecular weight or process parameters were to be used. However for the specific experimental conditions and polymer and solvent systems used in this study, it can give a reasonable prediction of the mean fibre diameter, and useful insight with regards to the influence of the fibre morphology. Fibres with beaded morphologies were not used as data for the development of the equation, since the presence of beads affects the fibre diameter. The equation that was developed is

$$D = 8435x_1^2 - 328.0x_1x_2 - 119.5x_1x_3 + 24483x_1 - 58.24x_2^2 + 4.670x_2x_3 + 3339x_2 + 0.2620x_3^2 - 187.8x_3 - 45920$$

where D is the predicted average diameter of the fibres (nm), x_1 is the solution conductivity (μS/cm), x_2 is the solution surface tension (mN/m), and x_3 is the solution

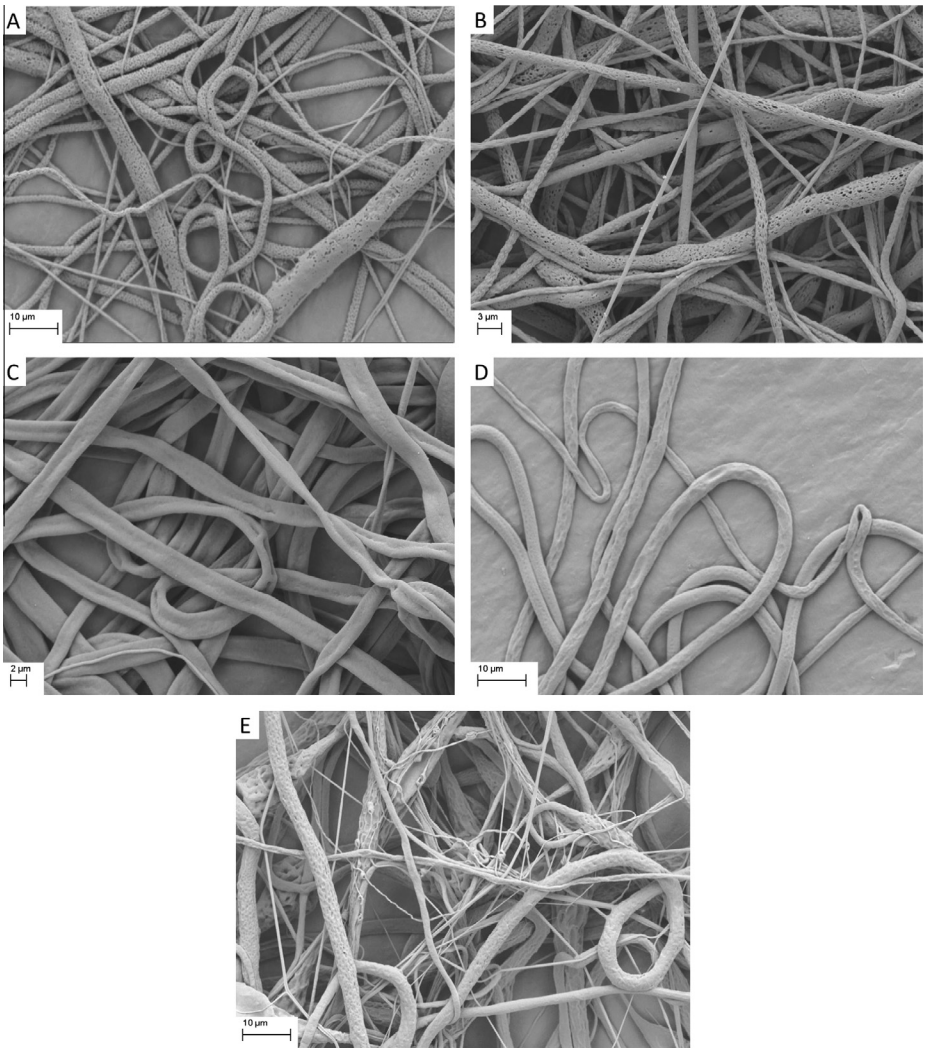

Fig. 8. SEM pictures of the fibres produced for the testing of the empirical equation. The good solvent and its amount in the solvent mixture was: (A) CF 75% *v*/*v*, (B) DCM 75% *v*/*v*, (C) DCM 83% *v*/*v*, (D) THF 75% *v*/*v*, and (E) THF 83% *v*/*v*.

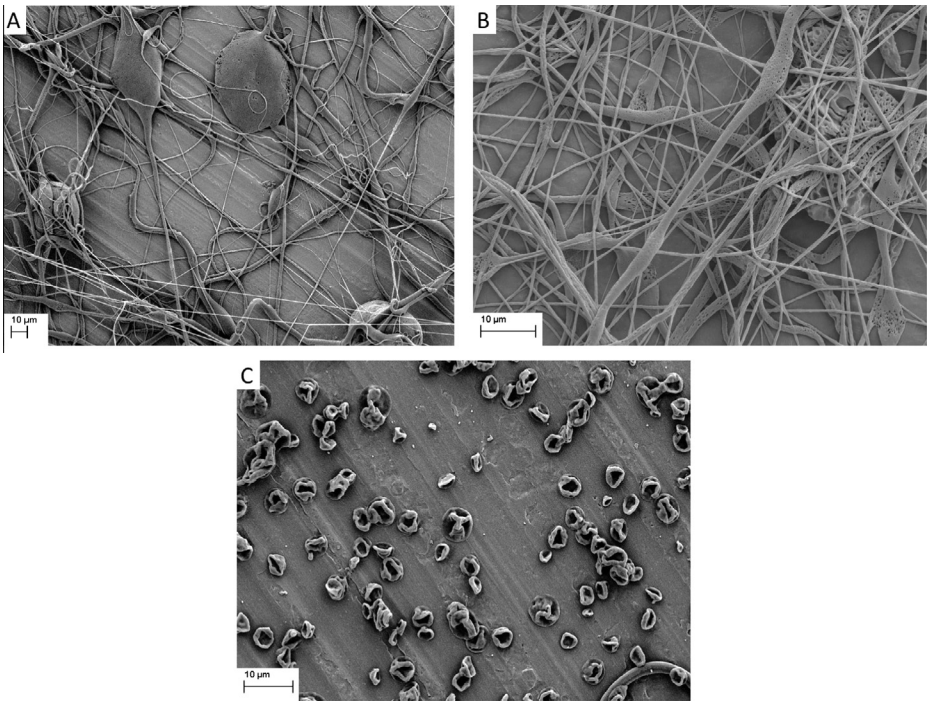

Fig. 9. SEM pictures of the fibres produced by 10% *w*/*v* CF/DMSO solutions. The good/poor solvent ratio was: (A) 90% *v*/*v*, (B) 75% *v*/*v*, and (C) 50% *v*/*v*.

viscosity (mPa s). The fitting of the experimental data in the empirical equation is shown in Fig. 6.

The equation was tested for 5 different samples produced with different good solvents and at different good solvent concentrations, for the specific experimental conditions used in this study and the results are demonstrated in Table 5 and Fig. 7. Production of bead free fibres was the main criterion for the selection of the good/poor solvent ratio. Fig. 8 shows the morphology of the fibres that were produced for the testing of the empirical equation.

The equation predicted quite accurately the produced fibre diameter for the cases where the amount of good solvent (CF and DCM) was 75% *v*/*v*. The predicted diameters were 1630 and 1420 nm respectively, whereas the experimental diameters were 1750 and 1290 nm. Larger deviation was observed between the predicted and experimental diameter (1850 and 2720 nm, respectively) for the case where the amount of DCM was 83% *v*/*v*. It should be noted that the as experimental diameter is characterised the width of the fibre and since the transition of the cross section from circular to ribbon consequences a diameter increase, the variation can, at least partially, be explained. The equation failed to predict the diameter of the fibres where the amount of THF was 75% *v*/*v* (predicted and experimental diameter 1320 and 2910 nm, respectively) and this could be due to the miscibility of THF with water and the subsequent increase of the surface tension. Nevertheless, it is an issue worth of further investigation. Finally, for the case where the amount of THF was 83% *v*/*v* the equation predicted diameter of 1610 nm, whereas the experimental diameter was 1280 nm.

3.3. Mapping the ternary composition region

The ternary system (polymer, solvent, non-solvent) that can be used for the production of porous, bead free fibres through the combination of electrospinning and phase separation should meet several requirements. The first requirement refers to the identification of the appropriate good solvent. As shown before, CF was proven to be a suitable solvent for the production of porous PCL fibres. CF has high enough evaporation rate compared to DMSO, so as to alter significantly the jet composition after its ejection, and low enough, so as not to favour skin formation.

The second requirement refers to the identification of the suitable good/poor solvent ratio. First of all, an amount of poor solvent has to be present in order to initiate the phase separation mechanism. However, it was demonstrated that the decrease of that ratio beyond a certain limit facilitates the formation of fibres with ribbon cross sections, which is in contrast with Qi et al. [27] findings. Qi et al. [27] used a binary solvent mixture of dichloromethane (solvent) and butanol (non-solvent) for the production of porous poly(L-lactic acid) fibres and reported that the increase of the good/poor solvent ratio favours pore formation. The differences can be attributed to the lower solution concentration that Qi used (8% *w*/*w* compared to 12.5% *w*/*v*), which does not hinder the motion of the polymer from the jet surface to the liquid core as strongly as in this study. In addition to that, Qi et al. [27] used butanol as a poor solvent, which is more volatile compared to DMSO (boiling points 118 and 189 °C, respectively). Thus, the amount of poor solvent, which also hinders the polymer diffusion to the core, was

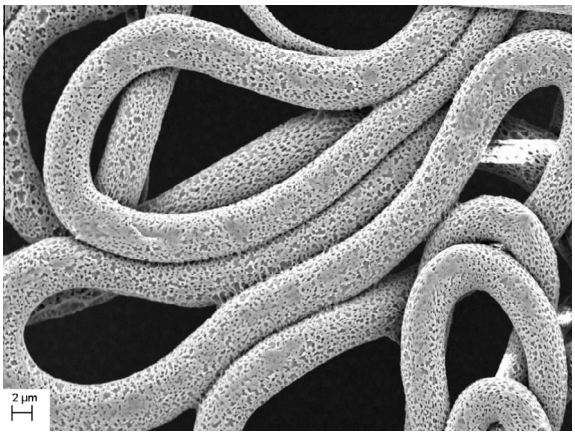

Fig. 10. SEM image of fibres produced by 15% *w*/*v* CF/DMSO solutions. The good/poor solvent ratio was 90% *v*/*v*.

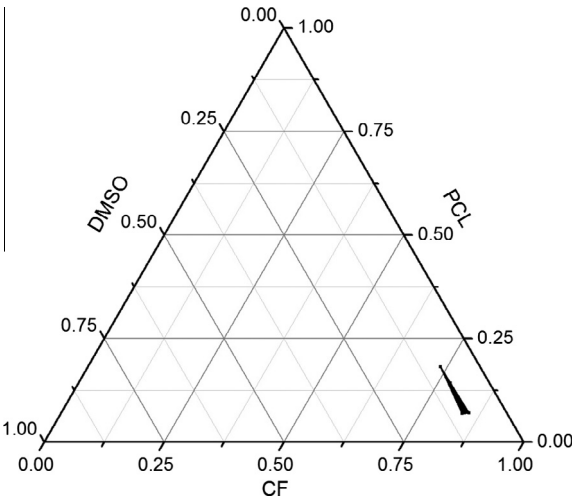

Fig. 11. Mapping of the region for the production of porous, bead free PCL fibres. The black shaded area indicates the ternary mixture compositions that can lead to the production of porous bead free PCL fibres.

decreased, and, therefore, the solid skin did not form. In the case of the 12.5% *w*/*v* CF/DMSO system, the good/poor ratio threshold for the skin formation lies at around 70% *v*/*v*.

The third requirement refers to the electrospinnability of the ternary system. In order to produce bead free fibres, the polymer amount has to be within the range where the, necessary for the fibre formation, chain entanglements within the electrospinning jet are achieved, but not excessive, so as to retain the produced fibre diameters at low levels.

The solution concentration effect was investigated by electrospinning of solutions with various concentrations. The 10% *w*/*v* solutions were proven to be unsuitable for the production of bead free fibre, regardless of the good/poor solvent ratio (Fig. 9). When the good/poor solvent ratio was 90% or 75% *v*/*v*, beads were observed on the fibres, whereas, a further increase of the poor solvent ratio (50% *v*/*v*) resulted the production of droplets. 12.5% *w*/*v* was shown to be a suitable polymer concentration for the production of bead free PCL fibres. In this case, the second requirement is met when the good/poor solvent ratio is held within the range of 75–90% *v*/*v*. When the solution concentration was further increased (15% *w*/*v*) porous, bead free fibres were produced, however, an enormous increase of the fibre average diameter was observed (around 4360 nm) (Fig. 10).

In summary, a ternary graph, indicating the regions where the process was successful, when CF was used as a good solvent was constructed, as shown in Fig. 11. The graph can be used to identify the regions under which the ternary system can result the production of porous, bead free fibres. It should be noted that the regions with higher polymer concentration were not investigated, since the concentration would further increase the fibre diameter.

4. Conclusions

The production of porous PCL fibres was achieved through a single step process by the addition of non-solvent to the polymer solution prior to electrospinning. The good solvent effect on the produced fibre morphology was investigated and CF was identified as a suitable solvent for that procedure. The evaporation rate of the good solvent is the parameter that determines its suitability, whereas, other properties, such as conductivity, surface tension and its miscibility with water affect the produced fibre morphology as well. The different fibre formation mechanisms that the jet undergoes under varying initial good/poor solvent ratios were explored and the emerging fibre morphologies were explained. An empirical equation correlating the produced fibre average diameter to the solution parameters (conductivity, surface tension, viscosity) was developed and tested. The regions, from which the ternary mixture can lead to the production of porous, bead free fibres, were identified.

References

[1] Bayley GM, Mallon PE. Porous microfibers by the electrospinning of amphiphilic graft copolymer solutions with multi-walled carbon nanotubes. Polymer 2012;53:5523–39.
[2] Bognitzki M, Frese T, Steinhart M, Greiner A, Wendorff J. Preparation of fibers with nanoscaled morphologies: electrospinning of polymer blends. Polym Eng Sci 2001;41:982–9.
[3] Casasola R, Thomas NL, Trybala A, Georgiadou S. Electrospun poly lactic acid (PLA) fibres: effect of different solvent systems on fibre morphology and diameter Polymer 2014;55:4728–37.
[4] Casper CL, Stephens JS, Tassi N, Chase DB, Rabolt JF. Controlling surface morphology of electrospun polystyrene fibers: effect of humidity and molecular weight in the electrospinning process. Macromolecules 2004;37:573–8.
[5] Demir MM. Investigation on glassy skin formation of porous polystyrene fibers electrospun from DMF. Express Polym Lett 2010;4:2–8.
[6] Doshi J, Reneker DH. Electrospinning process and applications of electrospun fibers. J Electrostat 1995;35:151–60.
[7] Fashandi H, Karimi M. Pore formation in polystyrene fiber by superimposing temperature and relative humidity of electrospinning atmosphere. Polymer 2012;53:5832–49.
[8] Formhals A. Process and apparatus for preparing artificial threads. U.S. Patent No. 1,975, 504; 1934.
[9] Georgiadou S, Thomas NL, Gilbert M, Brooks BW. Nonaqueous polymerization of vinyl chloride: an environmentally friendly process. J Appl Polym Sci 2009;112(4):2472–81.

[10] Guillen GR, Pan Y, Li M, Hoek EMV. Preparation and characterization of membranes formed by nonsolvent induced phase separation: a review. Ind Eng Chem Res 2011;50:3798–817.
[11] Gupta A, Saquing CD, Afshari M, Tonelli AE, Khan SA, Kotek R. Porous nylon-6 fibers via a novel salt-induced electrospinning method. Macromolecules 2009;42:709–15.
[12] Huang L, Bui N-N, Manickam SS, McCutcheon JR. Controlling electrospun nanofiber morphology and mechanical properties using humidity. J Polym Sci Part: Polym Phys 2011;49:1734–44.
[13] Kanani AG, Bahrami SG. Effect of changing solvents on poly(ε-caprolactone) nanofibrous webs morphology. J Nanomater 2011:724153.
[14] Koombhongse S, Liu W, Reneker DH. Flat polymer ribbons and other shapes by electrospinning. J Polym Sci: Part B Polym Phys 2001;39:2598–606.
[15] Koutroumanis KP, Holdich RH, Georgiadou S. Synthesis and micellization of a pH-sensitive diblock copolymer for drug delivery. Int J Pharm 2013;455(1):5–13.
[16] Laouini A, Koutroumanis KP, Charcosset C, Georgiadou S, Fessi H, Holdich RH, et al. pH-sensitive micelles for targeted drug delivery prepared using a novel membrane contactor method. ACS Appl Mater Interfaces 2013;5(18):8939–47.
[17] Lavielle N, Popa A-M, de Geus M, Hébraud A, Schlatter G, Thöny-Meyer L, et al. Controlled formation of poly(ε-caprolactone) ultrathin electrospun nanofibers in a hydrolytic degradation-assisted process. Eur Polym J 2013;49:1331–6.
[18] Lu P, Ding B. Applications of electrospun fibers. Recent Pat Nanotechnol 2008;2:169–82.
[19] Lubasova D, Martinova L. Controlled morphology of porous polyvinyl butyral nanofibers. J Nanomater 2011. 292516.
[20] Luo CJ, Stride E, Edirisinghe M. Mapping the influence of solubility and dielectric constant on electrospinning polycaprolactone solutions. Macromolecules 2012;45:4669–80.
[21] Martins A, Reis RL, Neves NM. Electrospinning: processing technique for tissue engineering scaffolding. Int Mater Rev 2008;53:257–74.
[22] Megelski S, Stephens JS, Chase DB, Rabolt JF. Micro- and nanostructured surface morphology on electrospun polymer fibers. Macromolecules 2002;35:8456–66.
[23] Murugan R, Ramakrishna S. Nano-featured scaffolds for tissue engineering: a review of spinning methodologies. Tissue Eng 2006;12:435–47.
[24] Nayani K, Katepalli H, Sharma CS, Sharma A, Patil S, Venkataraghavan R. Electrospinning combined with nonsolvent – induced phase separation to fabricate highly porous and hollow submicrometer polymer fibres. Ind Eng Chem Res 2012;51:1761–6.
[25] Nezarati RM, Eifert MB, Cosgriff-Hernandez E. Effects of humidity and solution viscosity on electrospun fiber morphology. Tissue Eng: Part C 2013;19:1–10.
[26] Pant HR, Neupane MP, Pant B, Panthi G, Oh H-J, Lee MH, et al. Fabrication of highly porous poly (ε-caprolactone) fibers for novel tissue scaffold via water-bath electrospinning. Colloids Surf., B 2011;88:587–92.
[27] Qi Z, Yu H, Chen Y, Zhu M. Highly porous fibers prepared by electrospinning a ternary system of nonsolvent/solvent/poly(L-lactic acid). Mater Lett 2009;63:415–8.
[28] Seo Y-A, Pant HR, Nirmala R, Lee J-H, Song KG, Kim HY. Fabrication of highly porous poly (e-caprolactone) microfibers via electrospinning. J Porous Mater 2012;19:217–23.
[29] Srinivasarao M, Collings D, Philips A, Patel S. Three-dimensionally ordered array of air bubbles in a polymer film. Science 2001;292:79–83.
[30] Van der Schueren L, De Schoenmaker B, Kalaoglu ÖI, De Clerck K. An alternative solvent system for the steady state electrospinning of polycaprolactone. Eur Polym J 2011;47:1256–63.
[31] Wei Z, Zhang Q, Wang L, Wang X, Long S, Yang J. Porous electrospun ultrafine fibers via a liquid–liquid phase separation method. Colloid Polym Sci 2013;291:1293–6.
[32] Woodruff MA, Hutmacher DW. The return of a forgotten polymer-polycaprolactone in the 21st century. Prog Polym Sci 2010;35:1217–56.